The feeding biomechanics and dietary ecology of *Australopithecus africanus*

David S. Strait[a,1], Gerhard W. Weber[b], Simon Neubauer[b,c], Janine Chalk[d], Brian G. Richmond[d,e], Peter W. Lucas[d], Mark A. Spencer[f], Caitlin Schrein[f], Paul C. Dechow[g], Callum F. Ross[h], Ian R. Grosse[i], Barth W. Wright[j], Paul Constantino[d], Bernard A. Wood[d,e], Brian Lawn[k], William L. Hylander[l], Qian Wang[m], Craig Byron[n], Dennis E. Slice[b,o], and Amanda L. Smith[a]

[a]Department of Anthropology, University at Albany, 1400 Washington Avenue, Albany, NY 12222; [b]Department of Anthropology, University of Vienna, Althanstrasse 14, A-1090 Vienna, Austria; [c]Department of Human Evolution, Max Planck Institute for Evolutionary Anthropology, Deutscher Platz 6, 04103 Leipzig, Germany; [d]Center for the Advanced Study of Hominid Paleobiology, Department of Anthropology, The George Washington University, 2110 G Street NW, Washington, D. C. 20052; [e]Human Origins Program, National Museum of Natural History, Smithsonian Institution, Washington, D. C. 20560; [f]School of Human Evolution and Social Change, Institute of Human Origins, Arizona State University, Box 874101, Tempe, AZ 85287-4104; [g]Department of Biomedical Sciences, Texas A&M Health Science Center, Baylor College of Dentistry, 3302 Gaston Avenue, Dallas, TX 75246; [h]Department of Organismal Biology and Anatomy, University of Chicago, 1027 East 57th Street, Chicago, IL 60637; [i]Department of Mechanical and Industrial Engineering, University of Massachusetts, 160 Governor's Drive, Amherst, MA 01003-2210; [j]Department of Anatomy, Kansas City University of Medicine and Biosciences, 1750 Independence Avenue, Kansas City, MO 64106-1453; [k]National Institute of Standards and Technology, Gaithersburg, MD 20899-8500; [l]Department of Biological Anthropology and Anatomy, Box 90383, Duke University, Durham, NC 27708-0383; [m]Division of Basic Medical Sciences, Mercer University School of Medicine, 1550 College Street, Macon, GA 31207; [n]Department of Biology, Mercer University, 1400 Coleman Avenue, Macon, GA 31207; and [o]Department of Scientific Computing, Florida State University, Dirac Science Library, Tallahassee, FL 32306-4120

Edited by David Pilbeam, Harvard University, Cambridge, MA, and approved December 12, 2008 (received for review September 2, 2008)

The African Plio-Pleistocene hominins known as australopiths evolved a distinctive craniofacial morphology that traditionally has been viewed as a dietary adaptation for feeding on either small, hard objects or on large volumes of food. A historically influential interpretation of this morphology hypothesizes that loads applied to the premolars during feeding had a profound influence on the evolution of australopith craniofacial form. Here, we test this hypothesis using finite element analysis in conjunction with comparative, imaging, and experimental methods. We find that the facial skeleton of the *Australopithecus* type species, *A. africanus*, is well suited to withstand premolar loads. However, we suggest that the mastication of either small objects or large volumes of food is unlikely to fully explain the evolution of facial form in this species. Rather, key aspects of australopith craniofacial morphology are more likely to be related to the ingestion and initial preparation of large, mechanically protected food objects like large nuts and seeds. These foods may have broadened the diet of these hominins, possibly by being critical resources that australopiths relied on during periods when their preferred dietary items were in short supply. Our analysis reconciles apparent discrepancies between dietary reconstructions based on biomechanics, tooth morphology, and dental microwear.

evolution | face | finite element analysis | hominin | diet

Feeding biomechanics evidently played an important role in shaping the evolution of hominin craniofacial form (1–4). Australopiths (an informal group subsuming Plio-Pleistocene hominins such as *Australopithecus* and *Paranthropus*) possess an adaptive complex including large postcanine (i.e., molar and premolar) tooth crowns covered with thick enamel; mandibles with large, robust bodies; exaggerated markings for the masticatory muscles; and substantial bony buttressing of the face. The enlargement of the premolar crowns (e.g., 5) is hypothesized to be biomechanically significant, because this trait implies that premolar loading was an important component of feeding behavior in these hominins (3). In most primates, the premolars are positioned anterior to the zygomatic root, so premolar bites should elevate stresses in the anterior rostrum (i.e., snout) where, typically, there are few derived stress-reducing traits that structurally reinforce the face. It is hypothesized that australopiths evolved features that buttress the face and reduce stress during premolar loading, including columns of bone positioned along either side of the nasal aperture (i.e., anterior pillars) and an anteriorly positioned and inferosuperiorly deep zygomatic root (3). Feeding behaviors that may have induced premolar loading and that are hypothesized to have been important in early hominins include the mastication of small, hard objects (2) or the mastication of high volumes of food spread across many teeth at once (6).

We tested hypotheses about premolar loading using finite element analysis (FEA) in conjunction with comparative, imaging, and experimental methods. FEA is an engineering technique used to examine how structures of complex design respond to external loads (7). In FEA, the structure of interest (e.g., a skull) is modeled as a mesh of simple bricks and tetrahedra (finite elements) joined at nodes, the elements are assigned material properties, certain nodes are constrained against motion, forces are applied, and stresses and strains at each node and within each element are calculated. Recent advances in computer software and imaging technology have made it possible to capture and digitally reconstruct skeletal geometry with great precision, thereby facilitating the generation of detailed finite element models (FEMs) of bony structures (8, 9). However, the incorporation of realistic muscle forces, bone material properties, modeling constraints, and experimental bone strain data are equally important components of FEA that are necessary to ensure biologically meaningful results (8, 10–12). We cannot collect these data for fossil taxa, so we assessed our modeling assumptions by comparing the strains derived from an FEA of an extant primate to those obtained from in vivo bone strain experiments (see SI). The strong correspondence between the FEA and experimental data suggests that our modeling assumptions are valid (10–12). This approach, in which FEA of fossils is informed by comparative and experimental data gathered from extant species, is currently the best means available for evaluating biomechanical hypotheses in extinct taxa.

Author contributions: D.S.S., G.W.W., B.G.R., M.A.S., P.C.D., C.F.R., I.R.G., and D.E.S. designed research; D.S.S., G.W.W., S.N., J.C., B.G.R., M.A.S., C.S., P.C.D., C.F.R., B.W.W., Q.W., and A.L.S. performed research; P.W.L., P.C., B.A.W., B.L., and W.L.H. contributed new reagents/analytic tools; D.S.S., G.W.W., B.G.R., P.W.L., M.A.S., P.C.D., C.F.R., I.R.G., B.W.W., Q.W., C.B., and D.E.S. analyzed data; and D.S.S., G.W.W., B.G.R., P.W.L., M.A.S., P.C.D., C.F.R., I.R.G., B.W.W., P.C., B.A.W., B.L., W.L.H., Q.W., C.B., and D.E.S. wrote the paper.

The authors declare no conflict of interest.

This article is a PNAS Direct Submission.

[1]To whom correspondence should be addressed. E-mail: dstrait@albany.edu.

This article contains supporting information online at www.pnas.org/cgi/content/full/0808730106/DCSupplemental.

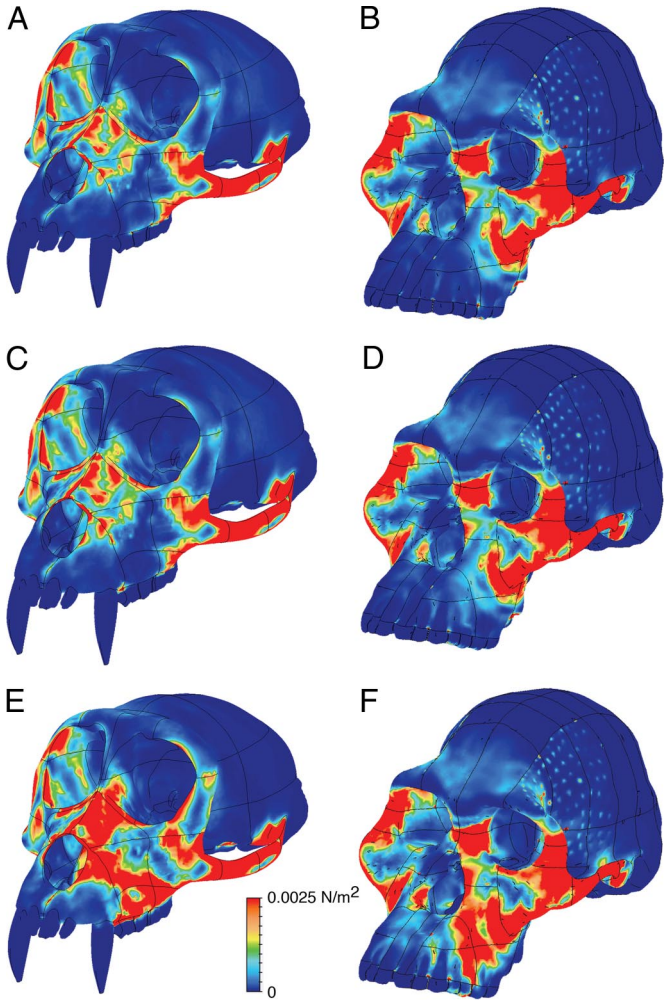

Fig. 1. Distributions of strain energy density (SED) observed in finite element analyses of *M. fascicularis* (*A*, *C*, *E*) and *A. africanus* (*B*, *D*, *F*) during simulated ''maximal'' bites on the molars alone (*A* and *B*), all of the postcanine teeth (i.e., the molars and the premolars) (*C* and *D*), and the premolars alone (*E* and *F*). SED distributions on the working (biting) side of the finite element models during ''maximal'' biting are nearly identical to those observed during ''normal'' biting, although magnitudes are lower in the latter. SED distributions are also nearly identical to those of Von Mises' strain in both models under all loading conditions, indicating that the strain energy stored in both crania is primarily distortional. With respect to size, the models are not drawn to scale.

We constructed FEMs (Fig. 1) of *A. africanus* and *Macaca fascicularis*. *A. africanus* is a "gracile" australopith exhibiting features of the facial skeleton hypothesized to resist elevated bite forces acting on the premolars (anterior pillars, zygomatic root positioned slightly anteriorly). The *A. africanus* model is a composite based on two specimens, Sts 5 and Sts 52, and is the first FEM and among the most complete virtual reconstructions to date of an australopith cranium. *M. fascicularis* is an extant monkey that lacks australopith facial features and whose feeding biomechanics has been the subject of intense study (e.g., 13). Thus, it is the species for which the most complete set of data on muscle architecture and activity as well as bone material properties and in vivo strain patterns could be collected.

To assess the biomechanical consequences of premolar loading, analyses were performed on each FEM in which the bite point was positioned first on the occlusal surfaces of the molars (M^1–M^3), then on the premolars (P^3–P^4), and then collectively on all of the postcanine teeth (i.e., on the molars and premolars simultaneously [P^3–M^3], as might occur when a large volume of food is being consumed during each bite; see SI for additional details). Two sets of muscle forces were applied for each bite point, one simulating a bite on a soft fruit (a "normal" bite) and the other on a highly stress-limited object (14) like a nut or seed (a "maximal" bite). Comparisons among the strain distributions in the FEMs allow an assessment of the biomechanical consequences of bite point position, muscle activity levels, and the function of skeletal traits.

Results and Discussion

In all analyses (Fig. 1), more of the facial skeleton of *A. africanus* is highly strained than that of *M. fascicularis*, suggesting that the facial morphology of *A. africanus* is more strongly influenced by masticatory forces. With respect to premolar biting, the elevation of strain energy density (SED) and Von Mises' strain (VMS) along the nasal margins in both models during normal and maximal biting (Fig. 1 *E* and *F*) suggests that the distribution of bone in this region is biomechanically and adaptively significant (3). Notably, the relatively high SED and VMS recorded on the anterior pillars of the *A. africanus* model suggest that the absence or reduction of these pillars might increase strains to the detriment of feeding behavior in this early hominin. High SED and VMS in the root of the zygoma, especially in *A. africanus*, also imply a significant role for this feature during feeding (3) and suggest that an investigation of the comparative bone structure of this feature in primates is warranted. In contrast, SED and VMS are consistently low in the browridges of both FEMs regardless of bite point location, suggesting that variation in browridge size and shape has little impact on feeding performance (13, 15). In both FEMs, SED and VMS patterns during biting on all of the postcanine teeth are nearly identical to those obtained during molar biting alone (Fig. 1 *A–D*), suggesting that a high volume diet (6) does not require stress-reducing buttressing of the facial skeleton over and above that required for mastication on the molars and, thus, that such a diet is unlikely to explain the evolution of these aspects of australopith facial form.

The *A. africanus* and *M. fascicularis* models behave similarly during premolar biting insofar as they both exhibit elevated SED and VMS on the working (biting) side rostrum above the premolars, along the nasal margin, and on the dorsal surface of the rostrum leading to the pillar of bone between the orbits. However, these similarities mask important differences in how the faces of these two species deform in response to premolar loads. In *A. africanus*, strains in these regions are dominated by compression (Fig. 2*B*, *D*), while in *M. fasicularis*, there are high concentrations of both tension and compression (Fig. 2*A*, *C*). At certain locations in *M. fascicularis*, tension and compression are nearly evenly balanced and when principal tensile and compressive strains are of equal magnitude at the same point, then the material at that point is in a state of pure shear. These interspecific differences in the relative proportions of tension and compression (i.e., in the principal strain ratio) are observed in all analyses regardless of variations in bite point position and muscle force magnitude (Table 1), suggesting that they are due primarily to structural differences in skeletal geometry. Moreover, principal strain ratios vary within and between regions to a much greater degree in *M. fascicularis* than in *A. africanus*, indicating a more complicated pattern of deformation in the former. In *M. fascicularis*, the shell-like rostrum lacks an anterior pillar and projects far in front of the zygomatic and thus deforms in a complex fashion due to a pronounced combination of twisting, bending, and shear. In contrast, in *A. africanus*, compressive strains during premolar loading are oriented superiorly and posteriorly, running from the teeth up along the anterior pillar and in a similar direction from the dorsal rostrum to the interorbital pillar. Furthermore, principal tensile strains in the same regions are small. Thus, as predicted (3), the anterior pillar

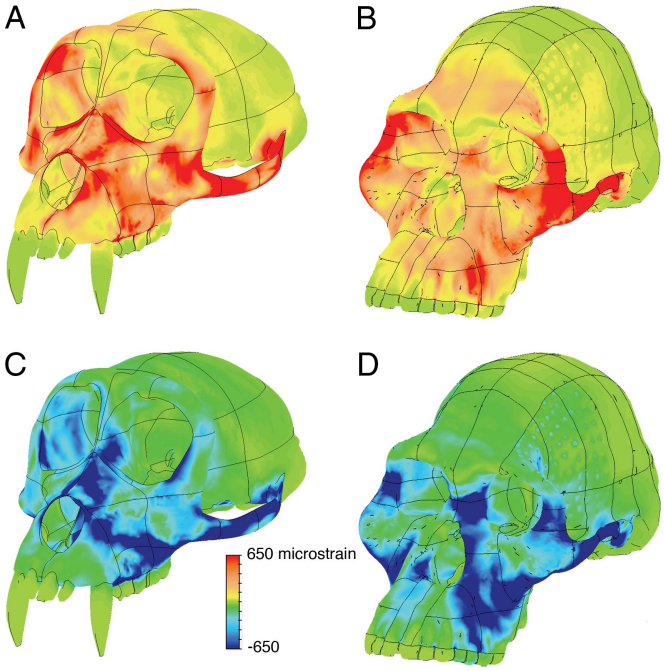

Fig. 2. Principal strains in the macaque and australopith models during ''maximal'' premolar biting. Maximum principal strain (*A* and *B*) representing tension and minimum principal strain (*C* and *D*) representing compression in *M. fascicularis* (*A* and *C*) and *A. africanus* (*B* and *D*).

acts as a strut, transmitting load in axial compression from the toothrow to the mid- and upper face and thereby minimizing the shear of the shorter rostrum against relatively anteriorly positioned zygomatics. Cortical bone, like many other ductile substances, is stronger in axial compression than in shear (16), indicating that facial skeleton of *A. africanus* is better designed to withstand premolar loads than that of *M. fascicularis.* Moreover, the fact that the rostrum experiences high strains only when the premolars are loaded in isolation is consistent with an hypothesis that the configuration of the *A. africanus* face is at least in part an adaptation to habitual premolar-focused biting, insofar as a strut would not be needed in the other loading regimes.

If the face of *A. africanus* evolved in part to withstand loads positioned specifically on the premolars, then what type of diet was involved? Stable carbon isotope analyses indicate that *A. africanus* had a diet that was isotopically mixed (e.g., 17), and the dental microwear on *A. africanus* molars indicates a varied diet consisting of a low incidence of hard foods, relatively nonresistant foods, and those that are displacement-limited (14) like tough vegetation (18). Dental microwear patterns in other ''gracile'' and some ''robust'' australopiths exhibit even less evidence of hard object feeding (19, 20), and none of the australopiths exhibit the extreme variability in microwear characterized by primates that seasonally exploit underground storage organs (19) like tubers. Among early hominins, only *Paranthropus robustus* exhibits microwear consistent with the regular and/or seasonal consumption of stress-limited foods (18). However, microwear-based evidence suggesting that hard foods were rare or absent in the diets of most australopiths is seemingly difficult to reconcile with dietary interpretations based on mechanics and comparative anatomy (2, 3, 6, 19–21). Thus, it has been suggested that, in some species, hard objects may have been ''fallback'' foods (i.e., less desirable foods that are eaten only when other preferred resources are not available [e.g., 22]) that were selectively important but infrequently consumed and thus may have influenced morphological evolution without leaving a microwear signal (19, 20). This hypothesis is viable but is difficult to test because it is based on negative evidence. Moreover, the hypothesis has not been applied to *A. africanus*, which is said to have relied on tough fallback foods (18) that were presumably displacement-limited. We propose an alternative, testable interpretation that resolves the apparent discrepancy between dietary reconstructions based on biomechanics and microwear.

We suggest, as have others (e.g., 21, 23), that australopith occlusal morphology is not well designed for processing tough, displacement-limited foods but instead represents an adaptation to eating stress-limited food items (14) such as seeds or nuts, in which a soft, nutritious core is mechanically protected by a hard outer casing (24). The casing is fractured by premolars (thereby explaining why buttressing of the face above the premolars is so important) and then is spat out, leaving the soft core to be masticated by the molars. The size of mechanically protected seeds, measured as an effective radius, typically ranges from 1–100 mm. However, the smallest of these seeds are unlikely to be the object of premolar biting. Bite forces at the premolars will be lower than or, at best, equal to those produced at the molars (25). Thus, given a small, stress-limited food object that can be

Table 1. Absolute values of ratios of maximum-to-minimum principal strain in the rostra of *A. africanus* and *M. fascicularis* in the six modeling analyses*

Species	Region†	Normal bite: molars	Normal bite: all cheek teeth	Normal bite: premolars	Maximal bite: molars	Maximal bite: all cheek teeth	Maximal bite: premolars
A. africanus	Lateral rostrum‡	0.73 (0.33)	0.64 (0.28)	0.67 (0.25)	0.76 (0.35)	0.67 (0.28)	0.69 (0.26)
	Nasal margin§	0.67 (0.35)	0.58 (0.30)	0.45 (0.16)	0.64 (0.34)	0.55 (0.29)	0.44 (0.17)
	Dorsal rostrum¶	0.37 (0.05)	0.37 (0.05)	0.39 (0.08)	0.38 (0.05)	0.37 (0.05)	0.38 (0.09)
	Interorbital pillar‖	0.47 (0.25)	0.47 (0.22)	0.45 (0.13)	0.46 (0.22)	0.46 (0.20)	0.45 (0.16)
M. fascicularis	Lateral rostrum	0.97 (0.64)	1.01 (0.66)	1.06 (0.66)	0.87 (0.63)	0.98 (0.68)	1.04 (0.64)
	Nasal margin	1.92 (1.34)	1.92 (1.36)	1.86 (1.35)	1.90 (1.30)	1.89 (1.32)	1.85 (1.33)
	Dorsal rostrum	0.84 (0.70)	0.82 (0.68)	0.66 (0.46)	0.78 (0.59)	0.75 (0.54)	0.61 (0.38)
	Interorbital pillar	1.03 (0.57)	1.01 (0.56)	0.57 (0.19)	1.04 (0.63)	0.98 (0.61)	0.56 (0.19)

*Mean (standard deviation). Values greater than 1.00 indicate that principal tensile strains exceed compressive strains, while values below 1.00 indicate the reverse.
†For each region, data were collected across multiple, evenly spaced nodes.
‡On the working (biting) side above the premolars and first molar.
§On the working (biting) side lateral to the nasal aperture, including the anterior pillar (in *A. africanus*).
¶On the working (biting) side superior and slightly lateral to the nasal aperture.
‖Between the orbits and extending slightly onto the medial surfaces of each orbit.

positioned at any point along the tooth row, there is no advantage to biting that object with the premolars, especially given that such bites elevate strains in the face. An alternative feeding behavior that might be the source of premolar loading is large, hard object feeding. A large food item is simply one that cannot be placed easily inside the oral cavity without first being processed by the teeth. Typically, anthropoids ingest large objects (e.g., fruits with soft mesocarps) with their incisors (26, 27), but when the food item is stress-limited, primates employ the less fragile canines and/or postcanine teeth (28). The molars would provide the highest bite force, but smaller gapes at molar bite points and interference from the soft tissues of the cheek would impede the processing of large objects. Because the premolars are positioned nearer the entrance of the mouth, and because gape is necessarily greater at the premolars than the molars, they could be used in the ingestion of larger stress-limited foods. We estimate maximum gape in *A. africanus* to be 50 mm at the premolars and 41 mm at the second molar (as determined by multiple regression of canine height and mandibular length onto maximum gape collected in vivo in a large sample of primates [29]), meaning that gape decreases at the more distal bite point by 18%. Moreover, molar gape probably overestimates maximum food particle size because, as noted, the cheek will inhibit the positioning of food items on the molar row (especially if parts of those items must protrude out of the mouth).

The processing of some large, hard food items may have entailed combining premolar biting with hand-assisted manipulation, as has been observed in extant primates in the wild (e.g., 28, 30) and during our in vivo experiments in the laboratory. Premolar-focused biting might also be associated with the ingestion of large, displacement-limited foods. One might hypothesize that the facial features examined here evolved in response to the frequent consumption of such items, but this hypothesis requires that skeletal adaptations to consuming displacement-limited foods evolved in australopiths without attendant dental adaptations. Thus, biomechanical considerations do not exclude the possibility that australopiths had a high volume diet or that they consumed smaller and/or displacement-limited items (31). Indeed, some aspects of australopith craniodental form may be adaptations to such diets (32). However, these diets do not provide the best explanation for the evolution of craniofacial features functionally related to premolar loading. Thus, large, stress-limited objects are likely to have been a selectively important component of a diet that may have otherwise been quite varied.

The ingestion of large, stress-limited objects with the premolars may explain the absence of a strong hard-object microwear signal in the molars of many australopiths (18–20). Given that premolars may well have been playing the key functional role in nut-cracking, we predict that molar microwear may not be detecting this behavior, and studies of premolar microwear are needed. Moreover, a new mechanical analysis (33) predicts that microwear features tend to be created only by grit and sufficiently hard but small food particles (i.e., less than roughly 5 mm in radius). Larger, mechanically protected seeds could have been eaten frequently, leaving little evidence on the premolar surface because dental damage would typically involve deep cracks initiating from the enamel-dentine junction and propagating outwards, rather than surface events. This hypothesis predicts that such deep cracks are present at an elevated frequency in the enamel caps of hard object feeders. The model further predicts that as the tooth crown thins due to wear (caused by the mastication of other types of food containing small abrasives), large, hard objects become even less likely to induce microwear. Moreover, the predicted lack of microwear is consistent with previously obtained experimental data (34) although more experimental evidence is needed, particularly pertaining to how grit adhering to seeds interacts with the seed and tooth surfaces as the seed is cracked. The absence of highly complex molar microwear textures in many australopiths (18–20) indicates that small, very hard objects were either rarely consumed, absent from the diet, or were not being eaten immediately before the deaths of the individuals whose bones became fossilized (e.g., individuals whose bones were interred as a result of water action may have died during a wet period when such foods were not needed). Microwear indicates that small, hard objects were part of the *P. robustus* diet (18), but we suggest on biomechanical grounds that *A. africanus* and perhaps other australopiths ingested large, hard foods with diameters ranging from approximately 10–50 mm. Several nut species that are seasonally available in modern African biomes fall in the middle of this size range (24). This interpretation is consistent with molar microwear analyses insofar as such analyses may have difficulty detecting the consumption of such items.

It has been hypothesized that some or all australopiths may have been ecological and dietary generalists (18, 21, 24, 35, 36). Our results indicate that key facial buttressing features in australopiths are adaptations for premolar biting, and insofar as these features may have allowed australopiths to process large foods that might have otherwise been inaccessible, they may have played a key role in facilitating a generalized diet. It is further possible that large, stress-limited nuts and seeds were among the fallback foods consumed by australopiths during periods when other, softer, preferred foods were unavailable. Given that australopiths experienced climates that were cooling and drying in the long term but which were variable in the short term (37), the need to periodically rely on fallback foods may have been critical (18, 21, 24, 35, 36). Australopith facial form is therefore likely to have been an ecologically significant adaptation.

Materials and Methods

Virtual Reconstruction and Surface Modeling of *A. africanus*. Sts 5 (38) was scanned in 1997 in Johannesburg, South Africa, with a medical CT (Siemens Somatom Plus 4, sequential, matrix x/y/z 512/512/130, voxelsize 0.39063/0.39063/1.0 mm, 140kV, 129mA). The scan is available at http://www.virtual-anthropology.com/3d_data/3d-archive. Despite its good preservation, reconstruction was required before biomechanical modeling. Using the Virtual Anthropology toolkit (39, 40) matrix was digitally removed from the orbits, the left and right zygomatic arches, the frontal and maxillary sinuses, the nasal cavity, the endocranial cavity, and the preserved root sockets by applying semiautomated (region growing) and manual segmentation. Plaster was also removed digitally. In most regions, the resulting gaps were reconstructed by mirroring intact contralateral parts. In some smaller regions on the cranial vault, gaps were filled using a smoothness of curvature criterion.

The tooth crowns of Sts 5 are missing, so they were reconstructed using Sts 52a. The latter was chosen because it derives from the same site (Sterkfontein) and stratigraphic layer (Member 4), is assigned to the same species (41), and, like Sts 5, is a subadult whose third molars are just erupting (42). The specimen was scanned in 2002 in Pretoria, South Africa, with a medical CT (Siemens Somatom Plus 4, sequential, matrix x/y/z 512/512/88, voxelsize 0.24219/0.24219/1.0 mm, 120kV, 60mA).

The teeth of Sts 52a, as well as the remains of the teeth (tooth roots) in the maxilla of Sts 5, were segmented. As Sts 52a is slightly compressed mediolaterally (43) and the teeth are better preserved on the right hemi dental arch than on the left, the former was mirrored to create a left tooth row. Both hemi dental arches were attached to the maxilla of Sts 5 to obtain a best-fit of root tips and preserved alveoli. The dental arch of Sts 52a fits without scaling to the maxilla of Sts 5.

The complete reconstructed geometry of the composite cranium was converted into a tessellated surface file (STL) for further implementation into the biomechanical modeling. Separate STL files were created for the maxillary and frontal sinuses, and for the nasal cavity. Using surface modeling software (Geomagic), any small-scale surface irregularities or artificial gaps in the internal and external geometry of the STL files were corrected following the bone's curvature resulting in new, smooth tessellated surfaces. These refined surfaces were then converted into Nonuniform Rational B-Spline (NURBS) surfaces that were then used to construct a solid *A. africanus* model. See SI for additional details.

Solid Modeling. The NURBS surface model of the external geometry of the *A. africanus* composite skull was imported into Solidworks software, made watertight, and then converted into a solid. The NURBS surfaces of the maxillary and frontal sinuses and the nasal cavity were subsequently imported and were used to cut cavities into the preexisting solid. Trabecular bone was modeled by defining surfaces corresponding to cancellous bone regions and then using those surfaces to define solids nested inside the rest of the skull. Thus, we modeled cancellous bone as a volume, as opposed to modeling individual trabeculae. As a simplifying assumption, soft tissue structures like the periodontal ligament and patent craniofacial sutures were not modeled because their incorporation would dramatically increase the complexity of the FEA. Our validation data (see below) suggest that even though these features are not included in our analyses, our FEMs are nonetheless sufficiently realistic to be useful in interpreting craniofacial biomechanics. The solid modeling of *M. fascicularis* is described elsewhere (12). See SI for additional details.

Finite Element Models. The solid models of *M. fascicularis* and *A. africanus* were imported into FEA software (Algor FEM Pro) and meshed using a combination of brick and tetrahedral elements. The *M. fascicularis* model contains 311,047 elements, while the *A. africanus* model contains 778,586 elements. The *M. fascicularis* model was assigned orthotropic material properties, which in the FEA software package requires the use of midside nodes. Midside nodes were not used in the *A. africanus* model, but that model is more densely meshed.

Material Properties. Cortical bone in the macaque was modeled orthotropically according to cranial region (44). We modeled cortical bone in *A. africanus* as being isotropic, and with values for elastic modulus and Poisson's ratio calculated as averages of the macaque values in the axis of maximum stiffness ($E = 17.319$ GPa, $v = 0.28$). Trabecular bone was assigned isotropic material properties by volume rather than by individual trabeculae following Ashman *et al.* (45) ($E = 637$ MPa, $v = 0.28$). Tooth enamel in the *A. africanus* FEM was assigned values following Kupczik *et al.* (46) ($E = 70$ GPa, $v = 0.3$). See SI for additional details.

Muscle Forces. The loads applied to the models comprise the forces of the eight major masticatory muscles whose activity peaks at or near centric occlusion: superficial masseter, deep masseter, anterior temporalis, and medial pterygoid muscles on the right and left sides. Muscle force magnitude in *Macaca* was estimated using a combination of simultaneous electromyography (EMG) data and measures of the physiological cross-sectional area (PCSA) of each muscle (12). Thus, muscle force asymmetry is included in the FEMs as is the lag time between the application of force and the detection of strain. EMG and PCSA cannot be observed in fossil hominins. As a first order approximation, PCSA data from a female specimen of *P. troglodytes* was used to estimate muscle force in *A. africanus.* Fasciculus length and angle of pinnation were determined for a sample of at least 10 fasciculi per muscle (47). The muscle bellies were then removed, excess connective tissue was dissected out, and the remaining tissue was weighed to the nearest 0.0001 g (Denver Instruments P-602). PCSA was calculated as PCSA (cm^2) = (muscle mass (gm) $\times$ cos θ)/(average fascicle length (cm) $\times$ 1.0564 gm/cm^3). We then applied EMG from *M. fascicularis* to our *A. africanus* FEM. The highest standardized root mean square EMG activity recorded from each electrode was assigned a value equal to 100% of the PCSA; when the muscle is acting below peak (e.g., at 50% of peak), then force is proportional to a corresponding percentage of PCSA. EMG data gathered simultaneously from the masticatory muscles enable the relative force magnitudes of each muscle to be estimated. Muscle force magnitudes were quantified as: F = (x-sectional area) X (300 kN/m^2) X (% of peak activity). See SI for additional details.

Constraints. The FEMs were constrained at evenly spaced nodes across both articular eminences and either the left premolars only, the molars only, or all of the postcanine teeth (molars and premolars). These constraints create reaction forces representing the joint and bite forces. See SI for additional details.

Validation. Strain data from FEA were compared to those gathered from in vivo chewing experiments on macaques and demonstrates (12) that our macaque model deforms in a realistic manner and is valid (see SI). Models of extinct taxa cannot be directly validated using in vivo techniques, but our *A. africanus* model was built using modeling assumptions equivalent to those used in the macaque model.

ACKNOWLEDGMENTS. We thank Francis Thackeray and Stephanie Potze from the Transvaal Museum, Northern Flagship Institution, Pretoria, South Africa, for access to fossils and the staff of Selby Clark Clinic, Johannesburg, South Africa, and the Little Company of Mary Hospital, Pretoria, South Africa, for the scanning of specimens. We also thank Gary Schwartz, Peter Ungar, and Frederick Grine for constructive discussions about enamel thickness, dental microwear, and diet. This project was funded by grants from the National Science Foundation Physical Anthropology HOMINID program (NSF BCS 0725219, 0725183, 0725147, 0725141, 0725136, 0725126, 0725122, 0725078) and the European Union FP6 Marie Curie Actions MRTN-CT-2005–019564 ''EVAN.''

1. Robinson JT (1954) Prehominid dentition and hominid evolution. *Evolution* 8:324–334.
2. Jolly CJ (1970) The seed eaters: A new model for hominid differentiation based on a baboon analogy. *Man* 5:5–26.
3. Rak Y (1983) *The Australopithecine Face.* (Academic, New York).
4. Lieberman DE, Krovitz GE, Yates FW, Devlin M, St. Claire M (2004) Effects of food processing on masticatory strain and craniofacial growth in a retrognathic face. *J Hum Evol* 46:655–677.
5. Grine FE (1988) in *Evolutionary History of the ''Robust'' Australopithecines*, ed Grine FE (Aldine de Gruyter, New York), pp 223–243.
6. Walker A (1981) Diet and teeth. *Phil Trans R Soc Lond B* 292:57–64.
7. Huiskes R, Chao EYS (1983) A survey of finite element analysis in orthopedic biomechanics: The first decade. *J Biomech* 16:385–409.
8. Rayfield EJ (2007) Finite element analysis and understanding the biomechanics and evolution of living and fossil organisms. *Ann Rev Earth Planet Sci* 35:541–576.
9. Macho GA, Shimizu D, Jiang Y, Spears IR (2005) *Australopithecus anamensis*: A finite element approach to studying the functional adaptations of extinct hominins. *Anat Rec* 283A:310–318.
10. Richmond BG, *et al.* (2005) Finite element analysis in functional morphology. *Anat Rec* 283A:259–274.
11. Ross CF, *et al.* (2005) Modeling masticatory muscle force in finite-element analysis: Sensitivity analysis using principal coordinates analysis. *Anat Rec* 283A:288–299.
12. Strait DS, *et al.* (2005) Modeling elastic properties in finite element analysis: How much precision is needed to produce an accurate model? *Anat Rec* 283A:275–287.
13. Hylander WL, Picq PG, Johnson KR (1991) Masticatory-stress hypotheses and the supraorbital region of primates. *Am J Phys Anthropol* 86:1–36.
14. Lucas PW, Turner IM, Dominy NJ, Yamashita N (2000) Mechanical defenses to herbivory. *Ann Bot (London)*86:913–920.
15. Kupczik K, Dobson C, Phillips R, Oxnard C, Fagan M, O'Higgins P (2009) Masticatory loading and bone adaptation in the supraorbital torus of developing macaques. *Am J Phys Anthropol,* in press.
16. Keyak JH, Rossi SA (2000) Prediction of femoral fracture load using finite element models: An examination of stress- and strain-based failure models. *J Biomech* 33:209–214.
17. Sponheimer M, Lee-Thorp JA (1999) Isotopic evidence for the diet of an early hominid, *Australopithecus africanus*. *Science* 283:368–370.
18. Scott RS, *et al.* (2005) Dental microwear texture analysis shows within-species diet variability in fossil hominins. *Nature* 436:693–695.
19. Grine FE, Ungar PS, Teaford MF, El-Zaatari S (2006) Molar microwear in *Praeanthropus afaensis*: Evidence for dietary stasis through time and under diverse paleoecological conditions. *J Hum Evol* 51:297–319.
20. Ungar PS, Grine FE, Teaford MF (2008) Dental microwear and diet of the Plio-Pleistocene hominin *Paranthropus boisei*. *PLoS ONE* 3:e2044.
21. Teaford MF, Ungar PS (2000) Diet and the evolution of the earliest human ancestors. *Proc Natl Acad Sci USA* 97:13506–13511.
22. Marshall AJ, Wrangham RW (2007) Evolutionary consequences of fallback foods. *Int J Primatol* 28:1219–1235.
23. Kay RF (1981) The nut-crackers—a new theory of the adaptations of the Ramapithecinae. *Am J Phys Anthropol* 55:141–151.
24. Peters CR (1987) Nut-like oil seeds: Food for monkeys, chimpanzees, humans, and probably ape-men. *Am J Phys Anthropol* 73:333–363.
25. Greaves WS (1978) The jaw lever system in ungulates: A new model. *J Zool (London)* 184:271–285.
26. Hylander WL (1975) Incisor size and diet in anthropoids with special reference to Cercopithecidae. *Science* 189:1095–1098.
27. Ungar PS (1994) Patterns of ingestive behavior and anterior tooth use differences in sympatric anthropoid primates. *Am J Phys Anthropol* 95:197–219.
28. Wright BW (2005) Craniodental biomechanics and dietary toughness in the genus *Cebus*. *J Hum Evol* 48:473–492.
29. Hylander WL, Vinyard CJ (2006) The evolutionary significance of canine reduction in hominins: Functional links between jaw mechanics and canine size. *Am J Phys Anthropol Suppl* 42:107.
30. Struhsaker T, Leland L (1977) Palm nut smashing by *Cebus apella* in Colombia. *Biotropica* 9:124–126.
31. Van der Merwe NJ, Masao FT, Bamford MK (2008) Isotopic evidence for contrasting diets of early hominins *Homo habilis* and *Australopithecus boisei* of Tanzania. *S Afr J Sci* 104:153–155.
32. Grine FE (1987) The diet of South African australopithecines based on a study of dental microwear. *L'Anthropologie* 91:467–482.
33. Lucas PW, Constantino P, Wood B, Lawn B (2008) Dental enamel as a dietary indicator in mammals. *BioEssays* 30:374–385.

34. Peters CR (1982) Electron-optical microscopic study of incipient dental microdamage from experimental seed and bone crushing. *Am J Phys Anthropol* 57:283–301.
35. Wood BA, Strait DS (2004) Patterns of resource use in early *Homo* and *Paranthropus*. *J Hum Evol* 46:119–162.
36. Sponheimer M, Passey BH, de Ruiter DJ, Guatelli-Steinberg D, Cerling TE (2006) Isotopic evidence for dietary variability in the early hominin *Paranthropus robustus*. *Science* 314:980–982.
37. Potts R (1998) Environmental hypotheses of hominin evolution. *Am J Phys Anthropol* 41:93–136.
38. Broom R (1947) Discovery of a new skull of the South African Ape-man, *Plesianthropus*. *Nature* 159:672.
39. Weber GW, *et al.* (2001) Virtual anthropology: The digital evolution in anthropological sciences. *J Physiol Anthropol Appl Human Sci* 20:69–80.
40. Neubauer S, Gunz P, Mitteroecker P, Weber GW (2004) Three-dimensional digital imaging of the partial *Australopithecus africanus* endocranium MLD 37/38. *Can Assoc Radiol J* 55:271–278.
41. Lockwood CA, Tobias PV (2002) Morphology and affinities of new hominin cranial remains from Member 4 of the Sterkfontein Formation, Gauteng Province, South Africa. *J Hum Evol* 42:389–450.
42. Thackeray JF, Braga J, Treil J, Niksch N, Labuscagne JH (2002) ''Mrs. Ples'' (Sts 5) from Sterkfontein: An adolescent male? *S Afr J Sci* 98:21–22.
43. Schwartz JH, Tattersall I (2005) *The Human Fossil Record*. Vol. 4: *Craniodental Morphology of Early Hominids (Genera* Australopithecus, Paranthropus, Orrorin*), and Overview* (John Wiley & Sons, Hoboken, NJ).
44. Wang Q, Dechow PC (2006) Elastic properties of external cortical bones in the craniofacial skeletons of the rhesus monkey. *Am J Phys Anthropol* 131:402–415.
45. Ashman RB, Cowan SC, Van Buskirk WC, Rice JC (1984) A continuous wave technique for measurement of the elastic properties of cortical bone. *J Biomech* 17:349–361.
46. Kupczik K, *et al.* (2007) Assessing mechanical function of the zygomatic region in macaques: Validation and sensitivity testing of finite element models. *J Anat* 210:41–53.
47. Anapol FC, Barry K (1996) Fiber architecture of the extensors of the hindlimb in semiterrestrial and arboreal guenons. *Am J Phys Anthropol* 99:429–447.